

Influence of Solvent on the Energetics of Hole Transfer in DNA

Julia A. Berashevich and Tapash Chakraborty*

Department of Physics and Astronomy, The University of Manitoba, Winnipeg, Canada, R3T 2N2

Received: July 3, 2007; In Final Form: August 2, 2007

We have investigated the contribution of molecular environment to the exchange reactions in the DNA molecule taking into account different geometries of the reaction centers in oxidized and reduced states. We have observed the influence of the ionization potential of the donor and the acceptor on the free energy of the hole transfer reaction in the solvated DNA molecule: A decrease of the free energy occurs if $IP_A \geq IP_D$ and an increase if $IP_A \leq IP_D$. The corresponding decrease of the potential barrier by 0.244 eV for hole migration from (G–C) to (A–T) and increase for migration from (G–C) to (G–C)_n in solvent have been determined. The prevalence of oxidation of the redox states in the molecule center in comparison to the molecule sides due to the nonuniform charge distribution along the phosphate backbone was found to be stronger for the non-neutralized backbone than for the neutralized case. The influence of the single counterion on the electrostatic interactions within the solute DNA molecule has been found to be smoothly spread over a long distance ~ 7 –8 base pairs. Therefore, each counterion contributes to the oxidation potential of the 7–8 nearest nucleosides and any irregularity due to phosphate neutralization would not significantly modify the potential profile for the hole migration through the DNA molecule.

I. Introduction

The discovery of charge transfer in the DNA molecule has opened a new avenue for nanoelectronics, where a double-helical structure of the DNA molecule can operate as molecular wire conducting the charge.^{1–9} However, the irregularity of the molecular structure, the high flexibility of the skeleton, and strong interactions with the surrounding environment make it difficult to predict the nature of charge migration in the DNA molecule.

The potential profile for the hole migration in the DNA molecule can be roughly determined by the difference of the ionization potential (IP) of the redox-active groups participating in reactions.¹⁰ However, the electrostatic interactions of the donor and the acceptor with the surrounding environment and the geometry fluctuations in the molecular structure accompany the transfer reaction and can produce significant changes in comparison to the IP difference.¹¹ It is a common procedure to include the geometry fluctuation and the environment contribution into the reorganization energies for charge-transfer simulations.¹² The response of the solvent environment is included in the solvent reorganization energy,^{2,10,13–15} whereas the geometry fluctuations of the reaction centers are incorporated into the inner-sphere reorganization energy. The inner-sphere reorganization energy has been experimentally estimated to be 0.6 eV, and the solvent reorganization energy is 0.3–0.5 eV.^{2,16}

Although the theoretical estimations of the IP values^{7,8} and the inner-sphere reorganization energies¹⁷ agree with the experimental data, the magnitude of the solvent reorganization energy has serious inconsistency between the theoretical simulations^{10,13–15} and the experimental measurements.^{2,16} The simulated values are in the range of 1–3 eV^{10,13–15} against ~ 0.3 –0.5 eV in the experiments.^{2,16} Moreover, in the simulated results, an increase of the solvent reorganization energy with

increasing distance between the donor and the acceptor^{10,13–15} has been predicted, whereas the opposite or a practically distance-independent behavior was reported in different experiments for the DNA molecule.^{2,16} The commonly used approaches^{10,13–15} are based on Marcus' theory,¹² which deals with the donor and the acceptor intermediated by highly mobile solvent molecules, such as water molecules. Because of an increase of the number of water molecules reoriented due to the charge transfer, the solvent reorganization energy increases with the donor–acceptor separation in Marcus' theory. However, in the DNA molecule the donor and acceptor centers are separated by the molecular bridge, which is less flexible during the charge-transfer reactions. Therefore, the solvent reorganization energy in the DNA molecule should depend strongly on the properties of the molecular bridge. Moreover, the interaction of the initial and final states of the charge-transfer reaction with the surrounding environment can provide the energy shift of their potential surfaces that is not taken into account as yet in the literature.^{10,13–15}

Here, we accurately evaluate the contribution of the solvent environment into the charge-transfer reaction in the DNA molecule. This has been done within a method that takes into account the energy shift of the surfaces of the initial and final states due to their transfer from the vacuum into the molecular environment.

II. Method

In the DNA molecule, the charge migration occurs primarily with the participation of the DNA base pairs. The single step of the hole transfer between the donor (*D*) and the acceptor (*A*) is described by the exchange reaction $D^+ + A \rightleftharpoons A^+ + D$. The reaction itself includes several steps. Before reaction, the donor and the acceptor have electronic configurations of the reactants $D^+(X^+)$ and $A^0(X^0)$, where X^0 and X^+ correspond to the geometry conformation of the molecule. Just after the exchange reaction,

* Corresponding author. E-mail: tapash@physics.umanitoba.ca.

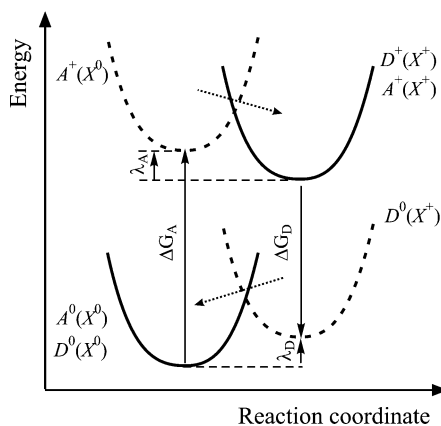
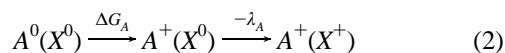
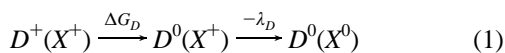


Figure 1. Schematic diagram for calculations of the reaction energies and the reorganization energies: for the acceptor – removing one electron from the neutral geometry $A^0(X^0)$ and for the donor – adding one electron to the positive ion $D^+(X^+)$.

the charge states of the donor and the acceptor are changed but the geometry configuration remains the same as before the reaction $D^0(X^+)$ and $A^+(X^0)$. They correspond to the intermediate states established within Marcus' theory.¹² The next step is the relaxation of the geometry of the reaction complexes to the final equilibrium states $D^0(X^0)$ and $A^+(X^+)$. Finally, the whole reaction processes are



where ΔG_D and ΔG_A are the free energies of the reduction (eq 1) and the oxidation (eq 2) processes; λ_D and λ_A are the reorganization energies. The summation of ΔG_D and ΔG_A gives the free energy of the exchange reaction, where the reorganization energy is also included

$$\Delta G = (E_{D^0(X^+)} - E_{D^+(X^+)}) + (E_{A^+(X^0)} - E_{A^0(X^0)}) \quad (3)$$

where $E_{A(D)^0(X^+)}$ is the energy of the neutral state in an ionic geometry, $E_{A(D)^+(X^+)}$ is the energy of the ionic state in an ionic geometry, $E_{A(D)^0(X^0)}$ is the energy of the neutral state in a neutral geometry, and $E_{A(D)^+(X^0)}$ is the energy of the ionic state in a neutral geometry. The differences $E_{A^+(X^0)} - E_{A^+(X^+)}$ and $E_{D^0(X^+)} - E_{D^0(X^0)}$ correspond to the reorganization energy. The scheme for calculation of the reorganization energies and the free energies is presented in Figure 1.

In the solvent, the redox-active groups interact not only with the surrounding solvent but also with other partial charges of the molecular polar groups. Because the phosphate group of each nucleotide carries a negative charge, the DNA molecule is highly soluble in water and strongly associates with both the water molecules and the positive ions. This provides the concentration of the positively charged counterions around the molecule in the surrounding solvent, while the DNA base pairs within the major or minor grooves can make the hydrogen-bonding links to the neutral water molecules.¹⁸ Therefore, for proper evaluation of the charge-transfer reaction in the DNA molecule the interactions of the donor and the acceptor with the neighboring redox-active groups, with the negatively charged sugar–phosphate backbones and the polar solvent environment, should be taken into account. All processes in the solute molecule during the charge-transfer reaction can be

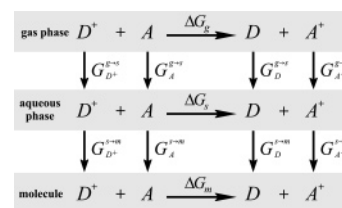


Figure 2. Thermodynamic cycle connecting the gas phase (g), the aqueous phase (s), and the molecule environment (m) for the exchange reaction between the donor and the acceptor.

divided into three general polarization modes in the gas and liquid phases, which weakly interact and can be evaluated separately.¹⁹ The electronic polarization takes care of the modification of the charge state and usually includes the high-frequency mode. Atomic polarization is a result of the nuclei displacement in response to the electronic polarization and is characterized by the low-frequency mode. The dipole polarization is the reorientation of the solute molecules according to the change of the electronic states of the reaction centers and correspond to the slower process in the molecular system.

In the vacuum, the electronic polarization of the reaction centers is included into the free energies $\Delta G_{g,D(A)}$. These energies correspond to the change of electronic configuration of the donor and acceptor during the reduction and oxidation reactions. The atomic polarization of the reaction centers, that is, the nuclei distortions in the donor and the acceptor geometries, are included in the $\lambda_{i,D(A)}$. Usually, the free energy $\Delta G^* = \text{aIP}_A - \text{aIP}_D$ between the equilibrium states, where aIP is the adiabatic IP, and the inner-sphere reorganization energy λ_i can be evaluated by the quantum chemical methods.¹⁷

Let us now describe the contribution from the surrounding medium. If the reaction centers are transferred from the vacuum into the molecular environment, then their potential energy surfaces are shifted because of the electrostatic interactions with the surrounding polar groups. The change of the charge state of the reaction centers leads to geometry fluctuations of the reaction center itself from (X^+) to the (X^0) geometries or vice versa and to the change of the electrostatic interactions with the surrounding environment. These interactions are mostly described by the degradation of the dipole polarization, while the electronic and the atomic polarizations of the surrounding environment can be disregarded. For example, it has been determined experimentally that substitution of some groups in the structure of the polyimide molecules provides a large change in the dipole polarization that dominates over the changes in the atomic part.¹⁹

In the past decade, the methodology for estimation of the energy shift to transfer the chemical reactions from the vacuum into the solution has been developed for titration of a protein.^{20–22} This methodology is represented by the thermodynamical cycle in Figure 2. The procedure includes two separate steps: transfer of the single redox-active group μ in different charge states from the vacuum to the aqueous solution $G_\mu^{g \rightarrow s}$ and then transfer to the molecular environment $G_\mu^{s \rightarrow m}$.

We have applied the methodology developed in refs 20–22 to describe the contribution of the surrounding medium for the exchange reaction in a DNA molecule. The free energy of the transfer reaction (see eq 3) in the solvent environment can be written as follows:

$$\Delta G_m = \Delta G_g^* + (\lambda_{i,A} + \lambda_{i,D}) + G^{g \rightarrow s} + G^{s \rightarrow m} \quad (4)$$

where

$$G^{s \rightarrow m} = G^{s \rightarrow s} + G^{s \rightarrow m} = G_D^{s \rightarrow m} - G_A^{s \rightarrow m} = (G_{D^0(X^+)}^{s \rightarrow m} - G_{D^+(X^+)}^{s \rightarrow m}) - (G_{A^0(X^0)}^{s \rightarrow m} - G_{A^+(X^0)}^{s \rightarrow m}) \quad (5)$$

If the single redox-active group μ is placed from the vacuum into the solution, then the energy shift $G_{\mu^0(\mu^+)}^{s \rightarrow s}$ is described by the solvation energy. The solvation energy of the redox-active group μ shows the electrostatic contribution of the polar solvent environment and based on the electrostatic potential computation in the aqueous phase (dielectric constant $\epsilon = 80$) and in the gas phase ($\epsilon = 1$)

$$G_{\mu^0(\mu^+)}^{s \rightarrow s} = \frac{1}{2} \sum_{i=1} q_i (\varphi(r)^{\epsilon=80} - \varphi(r)^{\epsilon=1}) \quad (6)$$

where $\varphi(r, \rho)$ is the electrostatic potential at the atomic position r , which is defined by the charge distribution $\rho(r)$ in an inhomogeneous dielectric medium within the Poisson–Boltzmann equation:

$$\nabla[\epsilon(r)\nabla\varphi(r)] = -4\pi\left(\rho(r) + \sum_{i=1} c_i^{\text{bulk}} q_i \exp\left(-\frac{q_i\varphi(r)}{k_B T}\right)\right) \quad (7)$$

Here c_i^{bulk} is the concentration of the ion i with the charge q_i in the bulk, and $\epsilon(r)$ is the dielectric constant at position r . For the exchange reaction between the molecular segments in the aqueous phase, the energy shift $G^{s \rightarrow s}$ contains the terms related to the oxidation and the reduction reactions (see eqs 3 and 5).

The next step is to estimate the energy required to transfer the redox-active groups μ from the aqueous solution into the molecular environment. The term $G^{s \rightarrow m}$ corresponds to the electrostatic response of the molecular environment for the change of the charge state at the donor ($\mu = D$) and acceptor ($\mu = A$) sides

$$G^{s \rightarrow m} = (G_{D^0(X^+)}^{s \rightarrow m} - G_{D^+(X^+)}^{s \rightarrow m}) - (G_{A^0(X^0)}^{s \rightarrow m} - G_{A^+(X^0)}^{s \rightarrow m}) \quad (8)$$

Here $G_{\mu^0(\mu^+)}^{s \rightarrow m}$ is the energy shift generated if the redox-active group μ is transferred from the aqueous solution into the molecular environment. The interactions of the redox-active group μ with the molecular and the solvent environment $G_{\mu}^{s \rightarrow m} = G_{\mu^0}^{s \rightarrow m} - G_{\mu^+}^{s \rightarrow m}$ are placed in three energy terms.²¹ The first term G_{μ}^{Born} describes the interaction of the charges of the group μ with its reaction field within the Born theory. The reaction field is the reorientation of the solvent polar molecules according to change of the electrostatic interactions as the result of the change of the charge state x_{μ}^n of the redox group μ from $x_{\mu}^n = 0$ to $x_{\mu}^n = 1$ ²¹

$$G_{\mu}^{\text{Born}} = \frac{1}{2} \sum_{i=1}^{N_{\mu}} Q_{i,\mu}^{\text{red}} [\varphi_m(r_i, Q_{i,\mu}^{\text{red}}) - \varphi_s(r_i, Q_{i,\mu}^{\text{red}})] - \frac{1}{2} \sum_{i=1}^{N_{\mu}} Q_{i,\mu}^{\text{oxd}} [\varphi_m(r_i, Q_{i,\mu}^{\text{oxd}}) - \varphi_s(r_i, Q_{i,\mu}^{\text{oxd}})] \quad (9)$$

Here the summations run over the N_{μ} atoms of group μ with charges $Q_{i,\mu}^{\text{oxd}}$ in the oxidized state and $Q_{i,\mu}^{\text{red}}$ in the reduced state. The electrostatic potential φ_m is caused by the charges of the oxidized and reduced states of the redox-active group μ inside the molecular environment, and φ_s is the single redox-active group in the solvent.

The second energy contribution G_{μ}^{back} represents the interactions of the redox-active group μ with the background charges of the polar solute. The charges of the atoms in the nonactive molecular groups and charges of the atoms in all of the active groups ν in their uncharged form denote the background charge q_i of the polar solute²¹

$$G_{\mu}^{\text{back}} = \sum_{i=1}^{N_m} q_i [\varphi_m(r_i, Q_{i,\mu}^{\text{red}}) - \varphi_m(r_i, Q_{i,\mu}^{\text{oxd}})] - \sum_{i=1}^{N_s} q_i [\varphi_s(r_i, Q_{i,\mu}^{\text{red}}) - \varphi_s(r_i, Q_{i,\mu}^{\text{oxd}})] \quad (10)$$

The first part of the equation is for the atoms N_m , which belong to the inactive or active groups ν in their uncharged form. The second summation runs over the atoms N_s of the redox-active group μ . These atoms have the same charge in the different charge states $x_{\mu}^n = 0$ and $x_{\mu}^n = 1$.

The redox behavior of the redox-active group strongly depends on the neighboring charges. Namely, if two redox-active groups are close to each other and are charged, then the coupling between them could be very strong. The interaction energies of the two groups μ and ν are given in the form of the W matrix. The electrostatic interaction $W_{\mu\nu}$ of the redox active groups μ and ν in their charged form is

$$W_{\mu\nu} = \sum_{i=1}^{N_{\mu}} [Q_{i,\mu}^{\text{red}} - Q_{i,\mu}^{\text{oxd}}] [\varphi_m(r_i, Q_{i,\mu}^{\text{red}}) - \varphi_m(r_i, Q_{i,\mu}^{\text{oxd}})] \quad (11)$$

Finally, the energy to transfer the exchange reaction from the aqueous phase to the solution $G^{s \rightarrow m}$ is included through the G_{μ}^{Born} , G_{μ}^{back} , and $W_{\mu\nu}$ energy terms as

$$G_{\mu}^{s \rightarrow m} = [G_{\mu}^{\text{Born}} + G_{\mu}^{\text{back}}] + \frac{1}{2} \sum_{\nu=1}^{N_{\nu}} W_{\mu\nu} x_{\mu}^n x_{\nu}^n \quad (12)$$

The last term in eq 12 appears when both groups μ and ν are in their charged states ($x_{\mu}^n = 1$, $x_{\nu}^n = 1$), otherwise $x_{\mu}^n = 0$ or $x_{\nu}^n = 0$. This term evaluates the probability of oxidation of the redox-active group μ in the molecule if group ν is already in the oxidized form. The summation runs over all of the redox-active groups ν in the molecule.

The procedure described above allows us to determine the free reaction energy between the two redox states in the aqueous phase and also in the solute based on the contributions from $G^{s \rightarrow s}$ and $G^{s \rightarrow m}$ energies, respectively. The $G^{s \rightarrow m}$ term, in comparison to the $G^{s \rightarrow s}$ energy, takes into account the change of electrostatic interactions between the states in the presence of the solute molecules characterized by the dielectric constant φ_s , which can differ from that in the aqueous phase. The details of the model can be found in ref 21.

We have used the approach presented above to evaluate the contribution of the solvent environment on the free energy of the exchange reactions between the redox-active groups in the DNA molecule (eq 4). First, the quantum chemical computations are performed in the vacuum to determine the optimized neutral and the ionic geometries of the redox-active groups and their atomic partial charge distribution. The geometries of the D^0 -, D^+ -, A^0 -, and A^+ -states have been determined in the Jaguar 6.5 program²³ within the Becke3P86/6-311+G* approximation of the DFT method. The RESP procedure²⁴ was applied for the optimized neutral and ionic geometries to determine the atomic partial charge of the redox-active groups. Second, the calculation of the solvent contribution into the ΔG_m is carried out by determining the $G^{s \rightarrow s}$ and $G^{s \rightarrow m}$ energy terms separately.

The optimized geometries of $D^0(X^+)$, $D^+(X^+)$, $A^0(X^0)$, and $A^+(X^0)$ states were used for electrostatic calculations in both the aqueous phase and the molecular environment. In the molecular environment, their geometries have been applied as bases for construction of the β -DNA chain.²⁵

The electrostatic interactions in the solute are evaluated by solving the Poisson–Boltzmann equation (eq 7) within the continuum electrostatic model, when the energy terms $G_{\mu(\mu^+)}^{g \leftrightarrow s}$, G_{μ}^{Born} , G_{μ}^{back} , and $W_{\mu\nu}$ can be obtained. According to this model,^{20–22} the molecule is represented as a continuum with a low dielectric constant, individual atomic partial charge, and the van der Waals radii. The solvent is represented as a continuum with a high dielectric constant, instead of the individual charges. The value of the dielectric constant within the molecule is a measure of the polarizability of the molecular systems, where the effect of the dielectric heterogeneity is included.^{26–29} The different mobilities of the molecular segments within the DNA chain can be described by the following dielectric constant: $\epsilon_1 = 3.4$ for the bases, $\epsilon_2 = 2.0$ for the sugar, and $\epsilon_3 = 20.6$ for the phosphate;²⁹ these values have been used in our calculations. Moreover, according to the experimental data, the dielectric behavior of the water molecules around the DNA base pairs (“bound water”) results in the dielectric constant being equal to 20 for the minor groove²⁸ and around 55²⁷ for the major groove. The deviation of the dielectric constant in the “bound water” zone from the bulk value arises because of the lower mobility of the solvent molecules, which are significantly polarized and constrained by the polar groups of the DNA. In our calculations, the dielectric constants have been increased gradually from the value $\epsilon_4 = 40$ in the “bound water” zone up to the dielectric constant $\epsilon_5 = 78.3$ in the bulk water within the interval of 3.0 Å.²⁹ For this purpose, the harmonic average smoothing method has been applied.

The general procedure for the electrostatic potential calculations applied in the last few decades was to evaluate the linearized Poisson–Boltzmann equation.^{20,22} However, the linearized form is valid for small electrostatic potentials ($q\varphi(r)/k_B T < 1$),²¹ which is not appropriate for a DNA molecule with negatively charged phosphate backbones. Therefore, in this paper the APBS program with a nonlinear three-dimensional Poisson–Boltzmann solver (eq 7) has been used to evaluate the electrostatic potential of the solute molecule.³⁰ The program has been improved to perform the G_{μ}^{Born} , G_{μ}^{back} , and $W_{\mu\nu}$ energy calculations and also has been adapted to take into account the zones with different dielectric constants. The high-resolution grid with the step of 0.25 Å centered at the redox-active group has been applied for the calculations. The van der Waals radii of the solvent molecule atoms have been used from parameter files for the DNA molecule.³¹ The salt concentration in the solvent was taken to be 0.1 M.

The Poisson–Boltzmann procedure has been successfully applied earlier for estimation of the solvent contribution into the free energy for simple molecular geometries and for proteins.³² In our work, we can use different dielectric constants for different molecular groups, which provides an improvement in the accuracy of our calculations of large molecules such as DNA. In our previous paper,¹¹ we found a good agreement of the computed solvation energy of the nucleobases with other theoretical results and the experimental data. As a result, our present model offers a reliable estimate of the contribution of the solvent environment on the free energy of the hole transfer reactions in the DNA molecule.

TABLE 1: Energy Shifts $G_A^{g \leftrightarrow s} = G_{A^+(X^0) \rightarrow A^0(X^0)}^{g \leftrightarrow s}$, $G_D^{g \leftrightarrow s} = G_{D^+(X^+) \rightarrow D^0(X^+)}^{g \leftrightarrow s}$, $G^{g \leftrightarrow s} = G_D^{g \leftrightarrow s} - G_A^{g \leftrightarrow s} = \lambda_A + \lambda_D$ (All Values Are in eV)

	aIP ^a	$G_A^{g \leftrightarrow s}$	$G_D^{g \leftrightarrow s}$	$G^{g \leftrightarrow s}$
guanine	7.75	0.866	0.850	−0.016
adenine	8.24	0.951	0.937	−0.014
cytosine	8.87	0.922	0.877	−0.045
thymine	9.14	1.112	1.128	0.016

^a All results are theoretical simulations.⁶

TABLE 2: Energy Shifts $G_{1 \rightarrow 2}^{g \leftrightarrow s} = G_{\mu=1(D)}^{g \leftrightarrow s} - G_{\mu=2(A)}^{g \leftrightarrow s}$ and $G_{2 \rightarrow 1}^{g \leftrightarrow s}$ (All Values Are in eV)

1/2	ΔG_g^*	$G_{1 \rightarrow 2}^{g \leftrightarrow s}$	$G_{1 \leftarrow 2}^{g \leftrightarrow s}$
adenine/thymine	0.5	−0.175	0.177
adenine/cytosine	0.4	0.015	−0.074
guanine/adenine	0.4	−0.101	0.071
guanine/thymine	0.9	−0.262	0.262
guanine/cytosine	0.8	−0.072	0.011
cytosine/thymine	0.1	−0.235	0.206

III. Numerical Results

A. Aqueous Phase. Nucleobases and their pairs are expected to be primarily redox-active groups participating in the charge-transfer reaction in the DNA molecule. The important issue for the redox-active groups in the aqueous phase is the energy change $G_{\mu}^{g \leftrightarrow s}$ during the oxidation and reduction reactions (see Figure 1) due to their transfer from the vacuum to the aqueous phase. The simulation results of $G_D^{g \leftrightarrow s}$ and $G_A^{g \leftrightarrow s}$ for separated nucleobases are presented in Table 1. The magnitude of the $G_{A(D)}^{g \leftrightarrow s}$ is found to be affected by the aIP value, in particular, the $G_{A(D)}^{g \leftrightarrow s}$ increases with increasing of the aIP; that is, the nucleobases with lower aIP can be easily oxidized as in vacuum as well as in the aqueous solution. For the exchange reaction between two states, the changes of the energy of the whole reaction due to transfer from the vacuum to the aqueous phase are included in the $G^{g \leftrightarrow s} = G_D^{g \leftrightarrow s} - G_A^{g \leftrightarrow s}$ energy term. The $G^{g \leftrightarrow s}$ energy can be compared with the solvent reorganization energy for the exchange reaction between two identical nucleobases. The magnitude of this energy is really small (see Table 1), and the energies to oxidize a neutral state and to reduce an oxidized state are practically equal to each other.

However, if the two states have different geometries, then the energies to reduce and oxidize these two states can be significantly different. The values of the reaction energy for the exchange reaction between two different nucleobases in vacuum ΔG_g^* and shift of the reaction energy in the aqueous solution $G^{g \leftrightarrow s}$ are presented in Table 2. As we can see, the solvent contribution results in a decrease or an increase of the free energy in the solvent depending on $G_{1 \rightarrow 2}^{g \leftrightarrow s}$ being negative or positive. The solvent decreases the energy gap for hole transfer from the adenine, the guanine, or the cytosine to the thymine. We can discern a common rule that usually the aqueous solution decreases the free energy of the exchange reaction for charge transfer between two different nucleobases if $\text{aIP}_A \geq \text{aIP}_D$ and increases if $\text{aIP}_A \leq \text{aIP}_D$.

During the charge-transfer reaction in DNA the charge can be localized on the nucleobase, DNA base pair and be delocalized over several base pairs in case of the polaron formation.^{3,33,34} In the next step, we are going to estimate the influence of the aqueous phase on the reduction and the oxidation processes if one, two, or three base pairs become a redox-active group μ . The results for the energy shifts $G_A^{g \leftrightarrow s}$, $G_D^{g \leftrightarrow s}$ and energy $G^{g \leftrightarrow s}$ for the $(G-C)_n$ and the $(A-T)_n$

TABLE 3: Energy Shifts $G_A^{g \rightarrow s}$ and $G_D^{g \rightarrow s}$ (All Values Are in eV)

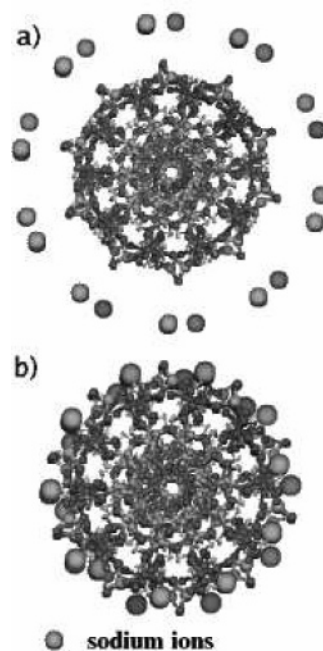
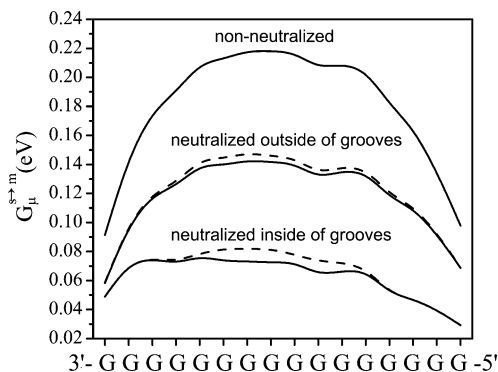
	aIP	$G_A^{g \rightarrow s}$	$G_D^{g \rightarrow s}$
(A-T) ₁	8.35	0.649	0.672
(A-T) ₂	8.11	0.415	0.445
(A-T) ₃	7.89	0.339	0.286
(G-C) ₁	7.71	0.571	0.485
(G-C) ₂	7.18	0.202	0.101
(G-C) ₃	6.89	0.039	0.047

oligomers are presented in Table 3. Clearly, stretching of the charge over the oligomer structure significantly decreases the aIP value and the $G_D^{g \rightarrow s}$, $G_A^{g \rightarrow s}$ energies. The decrease of the aIP value is related to the electron density distribution. In the aqueous phase, the dispersion of the unit charge over the larger geometry of redox states significantly decreases the positive charge concentration at the redox geometry edges and, therefore, decreases the force to reorientate the solute molecules and correspondingly the $G_\mu^{g \rightarrow s}$ value. The contribution of the aqueous phase on the transfer reaction between the (G-C) and the (A-T) states decreases the energy gap by 0.164 eV. This magnitude is larger in comparison to the value observed in the previous paper¹¹ because of the contribution in the present work of the geometry distortion during a transfer reaction.

B. Molecular Environment. In the molecular environment, the distance between the donor and the acceptor, the molecular bridge structure, the phosphate backbone, and the counterions neutralized phosphate backbone influence the charge migration process in the DNA molecule. Therefore, in this section we investigate their contributions to the $G_\mu^{s \rightarrow m}$ energy.

The molecular dynamics simulations³⁵ have shown that the positively charged ions in bulk water are highly mobile and, therefore, can strongly interact with the negatively charged phosphate backbone in the DNA molecule. The neutralization of the negative charge of the backbone by the counterions changes the electrostatic potential distribution over the whole DNA structure and modifies the oxidation potential of the nucleosides in the solvent. For example, in ref 35 the strong influence of the counterions to the charge-transfer reaction in the DNA molecule has been predicted. The important issue is the position of the counterions relating to the nucleosides. Within the quantum chemical computations, the location of the neutralized counterions was found to lie outside of the minor and major grooves of the DNA molecules.³⁶ However, the occurrence of the counterions in DNA grooves has been observed in the molecular dynamics simulations.³⁷ Therefore, we have simulated these two cases for the 3'-(G)₁₆-5' DNA sequences to study the influence of the counterion positions on the $G_\mu^{s \rightarrow m}$ energy. The simulated structures with explicitly defined ions are presented in Figure 3.

The separation of the counterions from the phosphorus atoms is 5.6 Å, which allows the water molecules to fill the space between them. The mobility of the counterions has been assumed to be equal to that for the water molecules within the "bound water" zone. The results for the $G_\mu^{s \rightarrow m}$ energy of the 3'-(G)₁₆-5' sequence when the phosphate is non-neutralized or neutralized inside or outside of the DNA grooves are presented in Figure 4. In the simulated results, the $G_\mu^{s \rightarrow m}$ energy has a maximum in the center of the molecule. The influence of the termination sides 5' and 3' is also observed, namely the value of $G_\mu^{s \rightarrow m}$ at the 3' side is higher than that at the 5' side. The charge distribution along the negatively charged phosphate backbones is nonuniform because of the lower density of the negative charge at the termination sides 5' and 3'. If the

**Figure 3.** Structure of 3'-(G)₁₆-5' sequence with sodium ions distribution: (a) ions are distributed outside of the DNA grooves; (b) ions are distributed inside of the major and minor grooves of the DNA molecule.**Figure 4.** Influence of the neutralization effect on the energy term $G_\mu^{s \rightarrow m}$ for the 3'-(G)₁₆-5' DNA chain. The dashed lines correspond to the neutralization pattern when the 8th guanine is not neutralized.

phosphate groups are non-neutralized, then the increase of the $G_\mu^{s \rightarrow m}$ energy in the molecule center occurs,¹¹ where the maximum density of the negative charge is localized. The nonuniformity of the negative charge distribution has a maximum close to the termination sides and decreases as one moves toward the molecule center and almost disappears for $n \geq 6$. We have introduced the $G_{1 \rightarrow 2}^{s \rightarrow m}$ term to estimate the contribution of the nonuniform charge distribution to the charge migration between the first and second base pair. For the non-neutralized backbone, the $G_{1 \rightarrow 2}^{s \rightarrow m}$ energy is found to be ~ -0.04 eV.

The neutralization of the phosphate by the counterions outside of the DNA grooves shifts the $G_\mu^{s \rightarrow m}$ curve for the non-neutralized case to lower energies and slightly reduces the maximum in the chain center, and as a result, $G_{1 \rightarrow 2}^{s \rightarrow m} \sim -0.02$ eV. The weak influence is related to the significant remoteness of the counterions from the redox-active group geometries. In the case of the location of the counterions inside the DNA grooves, the distance between the ions and the nucleosides is short. This leads to the downward shift of the $G_\mu^{s \rightarrow m}$ dependence along the energy axis and decreases the $G_{1 \rightarrow 2}^{s \rightarrow m} \sim -0.01$ eV. The influence of a single counterion on the electrostatic interactions

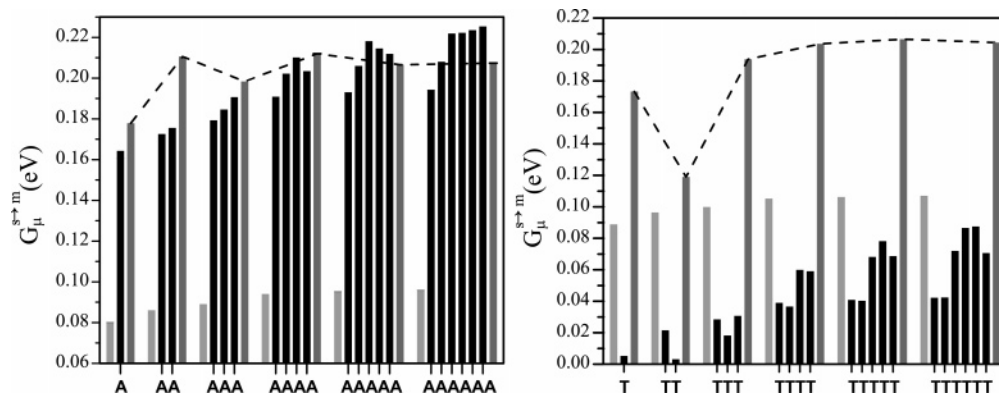


Figure 5. Dependence of G_{μ}^{s-m} energy on the geometries of the (a) 3'-(G-C)(A-T)_n(G-C)₃-5', (b) 3'-(G-C)(T-A)_n(G-C)₃-5' structures. The left gray bar corresponds to the 3'-(G-C) donor, the right gray bar to the (G-C)₃-5' acceptor. The dashed lines are guide to eyes only.

within the DNA molecule is extended over 7–8 base pairs and is stronger for neutralization within the DNA grooves (dashed lines in Figure 4). Therefore, if some of the phosphate backbone is non-neutralized, then the contribution of the nearest counterions neglects the influence of the negatively charged phosphate backbone on the G_{μ}^{s-m} energy.

In the DNA molecule, the fluctuations of the magnitude of the G^{s-m} energy in the case when the backbone is non-neutralized or neutralized are small in comparison to the G^{g-s} and the ΔG^g energies. Moreover, the neutralization effect can be included by the subtraction of its contribution from the G^{s-m} energy. For the charge-transfer reaction between the donor located on one side of the chain and the acceptor located on the other side, the contribution of the neutralization effect can be neglected. Therefore, for the following computational results we consider the DNA structure with a negatively charged phosphate backbone.

The next step is the investigation of the solvent contribution into the charge-transfer reaction between the (G-C), (G-C)₂, and (G-C)₃ traps intermediated by the molecular bridge (A-T)_n and (T-A)_n. The simulation results of the G^{s-m} energy are presented in Figure 5. According to these results, the elongation of the bridge length leads to an increase of the G_{μ}^{s-m} energy required to oxidize the redox-active states within a molecular structure. This is related to a decrease of the dielectric constant from $\epsilon_4 = 40$ in the bound-water zone for short molecules, when the space around the redox-active group is filled mostly by the highly mobile water molecules, to the values of ϵ_1 , ϵ_2 , and ϵ_3 for the long molecule. Therefore, for long DNA molecules the redox-active groups during the oxidation or reduction reactions are rigidly constrained by the surrounding redox groups. For the (G-C) → (G-C)₃ and (G-C)₂ → (G-C)₃ transfer the G^{s-m} energy is negative (~ -0.1 eV), whereas for the (G-C) → (G-C)₂ the G^{s-m} energy is close to zero. The deviation of the G_A^{s-m} energy (guided by the dashed lines in Figure 5) with expansion of the molecular bridge length occurs because of the helical structure of the DNA molecule, more precisely, the helical turn between different redox states.

IV. Discussion and Conclusions

On the basis of the simulation results, we conclude that the changes of the free energy of reactions ΔG_m in the molecular environment is mostly attributed to the G^{g-s} energy term whose contribution dominates over that from the G^{s-m} term.

The main effect of the aqueous solution into the G^{g-s} energy consists of a decrease of the free energy of reactions (ΔG_m) if $a\text{IP}_A \geq a\text{IP}_D$ and an increase if $a\text{IP}_A \leq a\text{IP}_D$ (see Table 2). The large energy gap between the donor and the acceptor in vacuum

TABLE 4: Contribution of the Gas Phase (ΔG_g^*), the Aqueous Phase (G^{g-s}), and the Molecular Environment (G^{s-m}) for Charge-Transfer Reactions in the DNA Molecule (All Values Are in eV)

	ΔG_g^*	G^{g-s}	G^{s-m}
(G-C)/(A-T)	0.53 ^a	-0.164	~ -0.08
(G-C)/(T-A)	1.4 ^a	-0.164	~ -0.08
(G-C)/(G-C) ₂	-0.47 ^a	0.283	~ 0.0
(G-C)/(G-C) ₃	-0.68 ^a	0.446	~ -0.1
(G-C) ₂ /(G-C) ₃	-0.21 ^a	0.062	~ -0.1

^a Theoretical simulations.⁶

causes the rise of the $|G^{g-s}|$ value, which in fact decreases this gap in the solvent. Therefore, the aqueous phase contribution decreases the free energy for charge transfer of the (G-C) → (A-T) states and increases for (G-C) → (G-C)₂, (G-C) → (G-C)₃, and (G-C)₂ → (G-C)₃ transfer reactions. The contribution of the aqueous and the solvent environment to the charge-transfer reactions in the DNA molecule is presented in Table 4. A significant change of the ΔG_m for the charge transfers (G-C) → (G-C)₂ and (G-C) → (G-C)₃ in comparison to the aIP difference in vacuum is supported by the experimental data, where the estimated free energies of these reactions in the solvent was found to be -0.008 – -0.055 eV and -0.077 eV, respectively.³⁸

For direct charge transfer between the donor and the acceptor separated by the (A-T)_n and (T-A)_n bridge, the contribution of the G^{s-m} energy term into the free energy of reactions ΔG_m is mostly provided by the phosphate backbone and the counterions, while the influence of the neighboring base pairs is not so significant. The nonuniform distribution of the negative charge over the phosphate backbones leads to an increase of G_{μ}^{s-m} in the structure center. Therefore, the positive charge is forced to migrate from the molecule sides to the center. A similar effect has been observed in the molecular dynamics simulations.³⁹ The neutralization of the phosphate backbone by the counterions decreases the maximum of the G_{μ}^{s-m} energy in the structure center (see Figure 4). The influence of the single counterion on the electrostatic potential distribution in the DNA molecule is smoothly extended over the 7–8 nearest base pairs. Therefore, because of the contributions from the nearest counterions alone the nonuniformity of the neutralization pattern would not dramatically change the potential profile for the hole migration through the DNA molecule. The prevalence of the contribution from the negatively charged phosphate backbone over the sequence pattern is in good agreement with the experimental data.³⁸ There, the shift of the donor (G-C) position by one sequence to the chain center and the shift of the acceptor

(G–C)₃ position by one sequence to the DNA side increases the reaction energy by 0.043–0.046 eV. This can be explained by the rise of the $G_{\mu}^{s \rightarrow m}$ energy in the center of the molecule. The variation of the sequence pattern nearest to the donor site changes the reaction energy only by 0.003–0.004 eV.³⁸

Let us consider the case of the solvent contribution for charge transfer from the donor to the acceptor carried out by the superexchange and the hopping mechanisms. According to the superexchange mechanism, the charge is not localized in the molecular bridge because of direct transfer from the donor to the acceptor. Therefore, the contribution of the molecular environment into the charge transfer is defined by the $G_{\mu}^{g \rightarrow s}$ and $G_{\mu}^{s \rightarrow m}$ energies for the donor and the acceptor. For the (G–C) → (G–C)₃ transfer, this is the positive shift 0.35 eV (see data in Table 4) that is slightly dependent on the distance between the donor and the acceptor. In the case of the hopping mechanism, when the charge can be localized on the bridge, $G_{(A-T) \rightarrow (A-T)}^{g \rightarrow s} = 0.023$ eV and $G_{(T-A) \rightarrow (T-A)}^{g \rightarrow s} = -0.014$ eV energies should be taken into account for the single transfer step (see data in Table 3). For the charge hopping over the 3'-(G–C)(A–T)_n(G–C)₃-5' structure the solvent contribution can be estimated by the $G^{g \rightarrow s}$ energy, while $G^{s \rightarrow m}$ can be neglected. Therefore, the next energies $G_{(G-C) \rightarrow (A-T)}^{g \rightarrow s} = -0.16$ eV, $G_{(A-T) \rightarrow (G-C)_3}^{g \rightarrow s} = 0.63$ eV and $n \cdot G_{(A-T) \rightarrow (A-T)}^{g \rightarrow s} = 0.023n$ eV should be taken into account. Finally, $G_{(G-C) \rightarrow (G-C)_3}^{g \rightarrow s} = (0.47 + 0.023n)$ eV. Similarly, for the 3'-(G–C)(T–A)_n(G–C)₃-5' structure the corresponding solvent effect is determined by $G_{(G-C) \rightarrow (G-C)_3}^{g \rightarrow s} = (0.47 - 0.014n)$ eV. The magnitude of the solvent contribution is close to the values of the solvent reorganization energies in the experimental data.² For the poly-(dA–dT) and poly(dG–dC) molecules, when the purine bases are the redox-active groups, the value of the $G_{(D) \rightarrow (A)}^{g \rightarrow s}$ decreases with elongation of the DNA chain because of the negative magnitude of the $G^{g \rightarrow s}$ energy (see Table 1). This result can explain the decrease of the reorganization energy observed in the experiment for the poly DNA molecules.¹⁶

In conclusion, the results obtained within our model presented here are in good agreement with the experimental results and explain some of the effects that could not be explained within the previous models.^{10,13–15} This shows the importance of including the shift of the potential surface of the redox groups in the solvent compared to their position in the vacuum.

Acknowledgment. This work has been supported by the Canada Research Chair Program and a Canadian Foundation for Innovation (CFI) Grant.

References and Notes

- (1) Ratner, M. A. *J. Phys. Chem.* **1990**, *94*, 4877–4883.
- (2) Lewis, F. D.; Kalgutkar, R. S. *J. Am. Chem. Soc.* **2000**, *122*, 12346–12351.
- (3) Conwell, E. *Top. Curr. Chem.* **2004**, *237*, 73–101.
- (4) Giese, B.; Amaudrut, J.; Köhler, A. K.; Spormann, M.; Wessely, S. *Nature* **2001**, *412*, 318–320.
- (5) Bixon, M.; Jortner, J. *J. Phys. Chem. A* **2001**, *105*, 10322–10328.
- (6) Sugiyama, H.; Saito, I. *J. Am. Chem. Soc.* **1996**, *118*, 7063–7068.
- (7) Voityuk, A. A.; Rösch, N.; Bixon, M.; Jortner, J. *J. Phys. Chem. B* **2000**, *104*, 9740–9745.
- (8) Troisi, A.; Orlandi, G. *Chem. Phys. Lett.* **2001**, *344*, 509–518.
- (9) Röche, S. *Phys. Rev. Lett.* **2003**, *91*, 108101.
- (10) LeBard, D. N.; Lilichenko, M.; Matyushov, D. V.; Berlin, Y. A.; Ratner, M. A. *J. Phys. Chem. B* **2003**, *107*, 14509–14520.
- (11) Berashevich, J. A.; Chakraborty, T. *J. Chem. Phys.* **2007**, *126*, 035104.
- (12) Marcus, R. A. *J. Chem. Phys.* **1956**, *24*, 966–978.
- (13) Tavernier, H. L.; Fayer, M. D. *J. Phys. Chem. B* **2000**, *104*, 11541–11550.
- (14) Tong, G. S. M.; Kurnikov, I. V.; Beratan, D. N. *J. Phys. Chem. B* **2002**, *106*, 2381–2392.
- (15) Siriwong, K.; Voityak, A. A.; Newton, M. D.; Rosch, N. *J. Phys. Chem. B* **2003**, *107*, 2595–2601.
- (16) Harriman, A. *Angew. Chem., Int. Ed.* **1999**, *38*, 945–949.
- (17) Olofsson, J.; Larsson, S. *J. Phys. Chem. B* **2001**, *105*, 10398–10406.
- (18) MacKerell, A. D., Jr.; Wiorkiewicz-Kuczera, J.; Karplus, M. *J. Am. Chem. Soc.* **1995**, *117*, 11946–11975.
- (19) Hougham, G.; Tesoro, G.; Viehback, A.; Chaplle-Sokol, J. D. *Macromolecules* **1994**, *27*, 5964–5971.
- (20) Harvey, S. C. *Proteins* **1989**, *5*, 78–92.
- (21) Ullmann, G. M.; Knapp, E.-W. *Eur. Biophys. J* **1999**, *28*, 533–551.
- (22) Bashford D.; Karplus M. *J. Phys. Chem.* **1991**, *95*, 9557–9561.
- (23) *Jaguar*, version 6.5; Schrödinger, LLC: New York, 2005.
- (24) Besler, B. H.; Merz, K. M.; Kollman, P. A. *J. Comput. Chem.* **1990**, *11*, 431–439.
- (25) Drew, H. R.; Wing, R. M.; Takano, T.; Broka, C.; Tanaka, S.; Itakura, K.; Dickerson, R. E. *Proc. Natl. Acad. Sci.* **1981**, *78*, 2179–2183.
- (26) Simonson, T.; Brooks, C. L. *J. Am. Chem. Soc.* **1996**, *118*, 8452–8458.
- (27) Barawakar, A.; Ganesh, K. N. *Nucleic Acids Res.* **1995**, *23*, 159–164.
- (28) Jin, R.; Breslauer, K. *Proc. Natl. Acad. Sci.* **1988**, *85*, 8939–8942.
- (29) Yang, L.; Weerasinghe, S.; Smith, P. E.; Pettitt, B. M. *Biophys. J.* **1995**, *69*, 1519–1527.
- (30) Baker, A. N.; Sept, D.; Joseph, S.; Holst, M. J.; McCammon, J. A. *Proc. Natl. Acad. Sci.* **2001**, *98*, 10037–10041.
- (31) MacKerell, A. D., Jr.; Banavali, N. *J. Comput. Chem.* **2000**, *21*, 86–104.
- (32) (a) Schmidt am Busch, M.; Knapp, E.-W. *Chem. Phys. Chem.* **2004**, *5*, 1513–1522. (b) Ishikita, H.; Saenger, W.; Biesiadka, J.; Loll, B.; Knapp, E.-W. *Proc. Natl. Acad. Sci.* **2006**, *103*, 9855–9860.
- (33) Schuster, G. B. *Acc. Chem. Res.* **2000**, *33*, 253–260.
- (34) Yoo, K.-H.; Ha, D. H.; Kee, J.-O.; Park, J. W.; Kim, J.; Kim, J. J.; Lee, H.-Y.; Kawai, T.; Choi, H.-Y. *Phys. Rev. Lett.* **2001**, *87*, 198102.
- (35) Barnett, R. N.; Cleveland, C. L.; Joy, A.; Landman, U.; Schuster, G. B. *Science* **2001**, *294*, 567–571.
- (36) Zhu, Q.; LeBreton, P. R. *J. Am. Chem. Soc.* **2000**, *122*, 12824–12834.
- (37) Korolev, N.; Lyubartsev, A. P.; Laaksonen, A.; Nordenskiöld, L. *Eur. Biophys. J.* **2004**, *33*, 671–682.
- (38) Lewis, F. D.; Liu, J.; Zuo, X.; Hayes, R. T.; Wasielewski, M. R. *J. Am. Chem. Soc.* **2004**, *125*, 4850–4861.
- (39) Voityuk, A. A.; Siriwong, K.; Rösch, N. *Angew. Chem., Int. Ed.* **2004**, *43*, 624–627.